Supplementary Materials

Machine-learning-assisted understanding of discontinuous precipitation behavior in Cu-Ni-Si alloy

Jinyu Liang[1,2], Fan Zhao[1,2,3,4,*], Guoliang Xie[5], Yu Lei[6], Ying Zhang[3], Xinhua Liu[1,2,4,6,*]

[1]Key Laboratory for Advanced Materials Processing (MOE), Institute for Advanced Materials and Technology, University of Science and Technology Beijing, Beijing 100083, China.
[2]Beijing Laboratory of Metallic Materials and Processing for Modern Transportation, Institute for Advanced Materials and Technology, University of Science and Technology Beijing, Beijing 100083, China.
[3]Beijing Advanced Innovation Center for Materials Genome Engineering, School of Advanced Materials Innovation, University of Science and Technology Beijing, Beijing 100083, China.
[4]Institute of Materials Intelligent Technology, Liaoning Academy of Materials, Shenyang 110167, Liaoning, China.
[5]State Key Laboratory for Advanced Metals and Materials, University of Science and Technology Beijing, Beijing 100083, China.
[6]Institute of Materials Genome Engineering, Henan Academy of Sciences, Zhengzhou 450046, Henan, China.

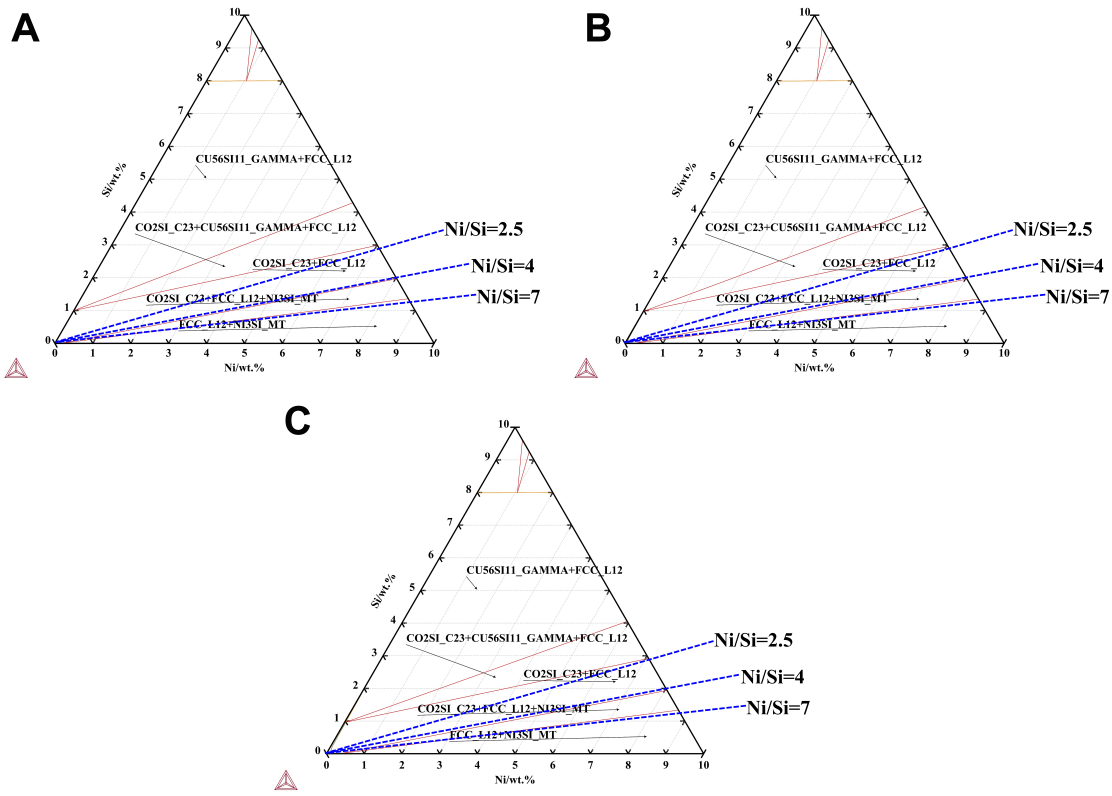
[*]**Correspondence to:** Dr. Fan Zhao, Prof. Xinhua Liu, Key Laboratory for Advanced Materials Processing (MOE), Institute for Advanced Materials and Technology, University of Science and Technology Beijing, Beijing 100083, China. E-mail: zhaofan@ustb.edu.cn; liuxinhua18@163.com

Supplementary Table 1. The orthogonal dataset of Cu-Ni-Si alloy at peak-aging stage

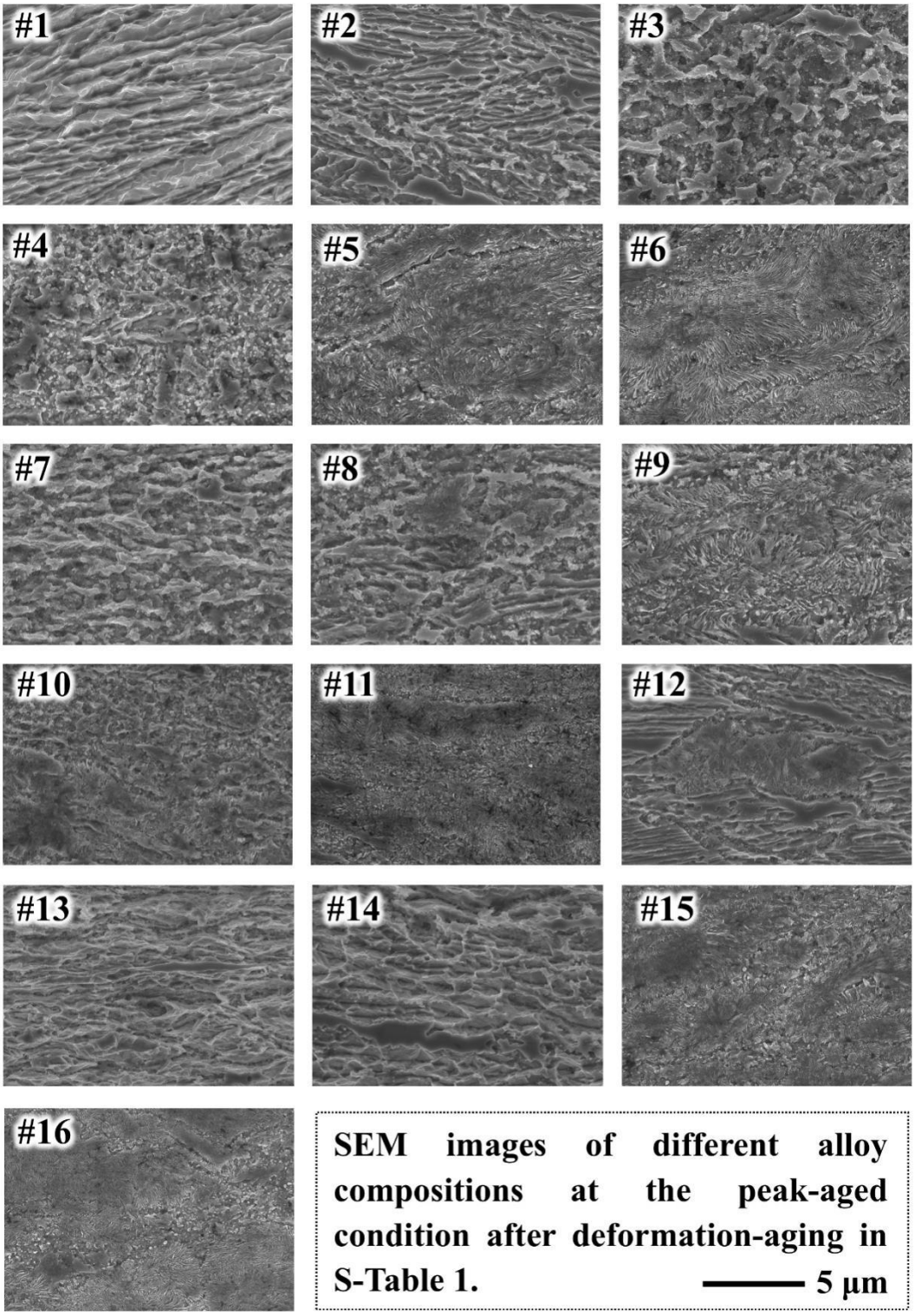
Number	Ni/wt.%	Si/wt.%	CR/%	AT/°C	at/h	EC/%IACS	Hardness/HV	DP occurrence	DP volume fraction/%
1	3	0.71	60	425	5	33.59	270.42	0	0
2	3	0.95	70	450	0.5	23.06	272.84	0	0
3	3	1.19	80	475	1	20.68	222.94	0	0
4	3	1.43	90	500	0.5	17.36	187.10	0	0
5	4	0.71	70	475	3	50.96	175.63	1	3.2
6	4	0.95	60	500	0.5	40.13	183.57	1	3.4
7	4	1.19	90	425	0.5	23.36	273.50	0	0
8	4	1.43	80	450	0.5	19.52	280.10	1	0.8
9	5	0.71	80	500	0.5	37.80	173.47	1	3.2
10	5	0.95	90	475	0.5	47.94	196.28	1	1.9
11	5	1.19	60	450	0.5	38.39	215.53	1	3
12	5	1.43	70	425	0.5	22.69	299.66	1	0.73
13	6	0.71	90	450	0.5	20.98	287.20	0	0
14	6	0.95	80	425	0.5	23.38	304.70	0	0
15	6	1.19	70	500	0.5	46.03	203.60	1	4.1
16	6	1.43	60	475	0.5	39.01	204.23	1	3.1

Notes: In the DPs column, a value of “0” denotes the absence of DPs, whereas a value of “1” signifies their presence.

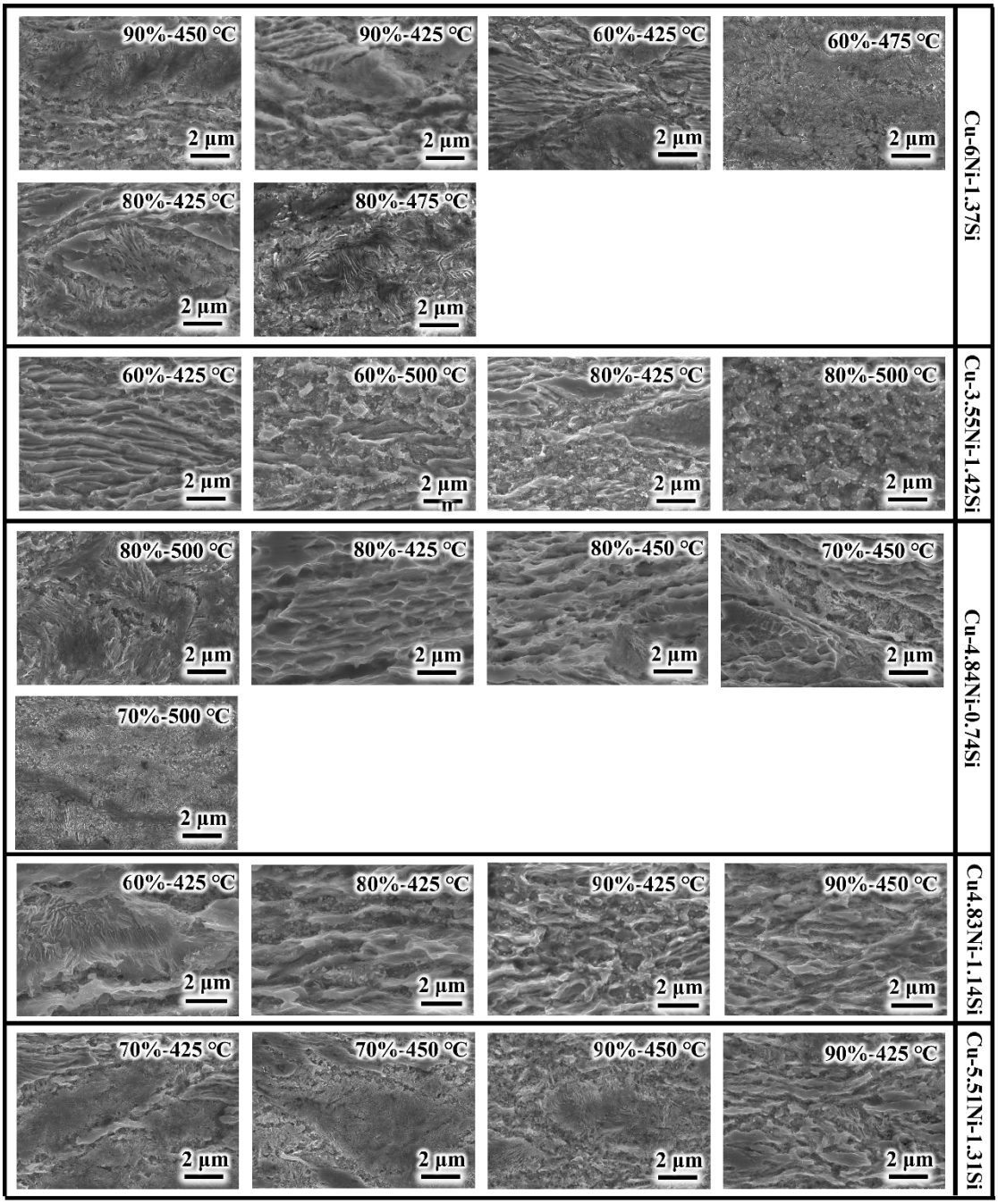
As shown in Supplementary Figure 1, the Ni and Si contents exert a pronounced influence on the types of precipitates formed in Cu-Ni-Si alloy. At a Ni/Si weight ratio above 7, Ni_3Si is the predominant precipitate in the matrix. When the Ni/Si weight ratio lies between 2.5 and 7, the precipitates consist primarily of Ni_2Si and Ni_3Si, whereas at ratios below 2.5, $Cu_{56}Si_{11}$ and Ni_2Si predominate. The precipitate phases vary in their capacity to enhance strength and also modify the residual concentrations of Ni and Si within the matrix, consequently influencing both the mechanical strength and electrical conductivity of the alloy. Previous studies have identified Ni_2Si and Ni_3Si as the principal strengthening precipitates in Cu-Ni-Si alloy, among which Ni_2Si is generally considered more favorable for achieving an optimal strength-electrical conductivity balance [S1–S3]. Accordingly, the Ni/Si weight ratio was constrained to 2.5–7 in the orthogonal compositional design. The ranges of Ni and Si contents were selected with reference to reported compositions of alloys containing DPs and high-solute alloys containing CPs [S4–S6]. The Ni content was therefore set to 3–6 wt.%, while the corresponding Si range was determined to be 0.71–1.43 wt.% based on the Ni/Si weight ratio range established by thermodynamic calculations.



Supplementary Figure 1. Phase diagram of Cu-Ni-Si alloy ternary isothermal section: (A-C) 425 ℃, 450 ℃ and 500 ℃, respectively.



Supplementary Figure 2. SEM images of different alloy compositions at the peak-aged condition after deformation-aging in Supplementary Table 1.



Supplementary Figure 3. SEM images of the samples corresponding to the validation results in Table 1.

REFERENCE

[S1] Lei, Q.; Li, S.; Zhu, J.; et al. Microstructural evolution, phase transition, and physics properties of a high strength Cu-Ni-Si-Al alloy. *Mater. Charact.* **2019**, *147*, 315-323. DOI: 10.1016/j.matchar.2018.11.018.

[S2] Yang, Z.; Qin, C.; Yu, Z.; et al. Precipitation thermodynamics, kinetics and mechanism of Cu-Ni-Si alloy modified by trace 0.1 wt.% P doping. *J. Mater. Res. Technol.* **2026**, *43*, 2834-2844. DOI: 10.1016/j.jmrt.2026.06.230.

[S3] Zhang, Y.; Wang, Z.; Zhao, S.; et al. Effect of Cr addition on microstructure and properties of Cu-Ni-Co-Si-Mg alloys. *J. Alloy. Compd.* **2026**, *1050*, 185684. DOI: 10.1016/j.jallcom.2025.185684.

[S4] Goto, M.; Yamamoto, T.; Han, S.; et al. Simultaneous increase in electrical conductivity and fatigue strength of Cu-Ni-Si alloy by utilizing discontinuous precipitates. *Mater. Lett.* **2021**, *288*, 129353. DOI: 10.1016/j.matlet.2021.129353.

[S5] Cao, Y.; Han, S.; Choi, E.; et al. Effect of inclusion on strength and conductivity of Cu-Ni-Si alloys with discontinuous precipitation. *J. Alloy. Compd.* **2020**, *843*, 156006. DOI: 10.1016/j.jallcom.2020.156006.

[S6] Ren, K.; Liao, X.; Pang, Y.; et al. Composition-driven fibrous-to-lamellar transition of discontinuous precipitates in Cu-Ni-Si alloys. *Mater. Des.* **2025**, *260*, 115102. DOI: 10.1016/j.matdes.2025.115102.